Appendix

Actin network architecture can ensure robust centering or sensitive decentering of the centrosome

Shohei Yamamoto, Jérémie Gaillard, Benoit Vianay, Christophe Guerin, Magali Orhant-Prioux, Laurent Blanchoin, Manuel Théry

Table of Contents

Appendix Fig. S1

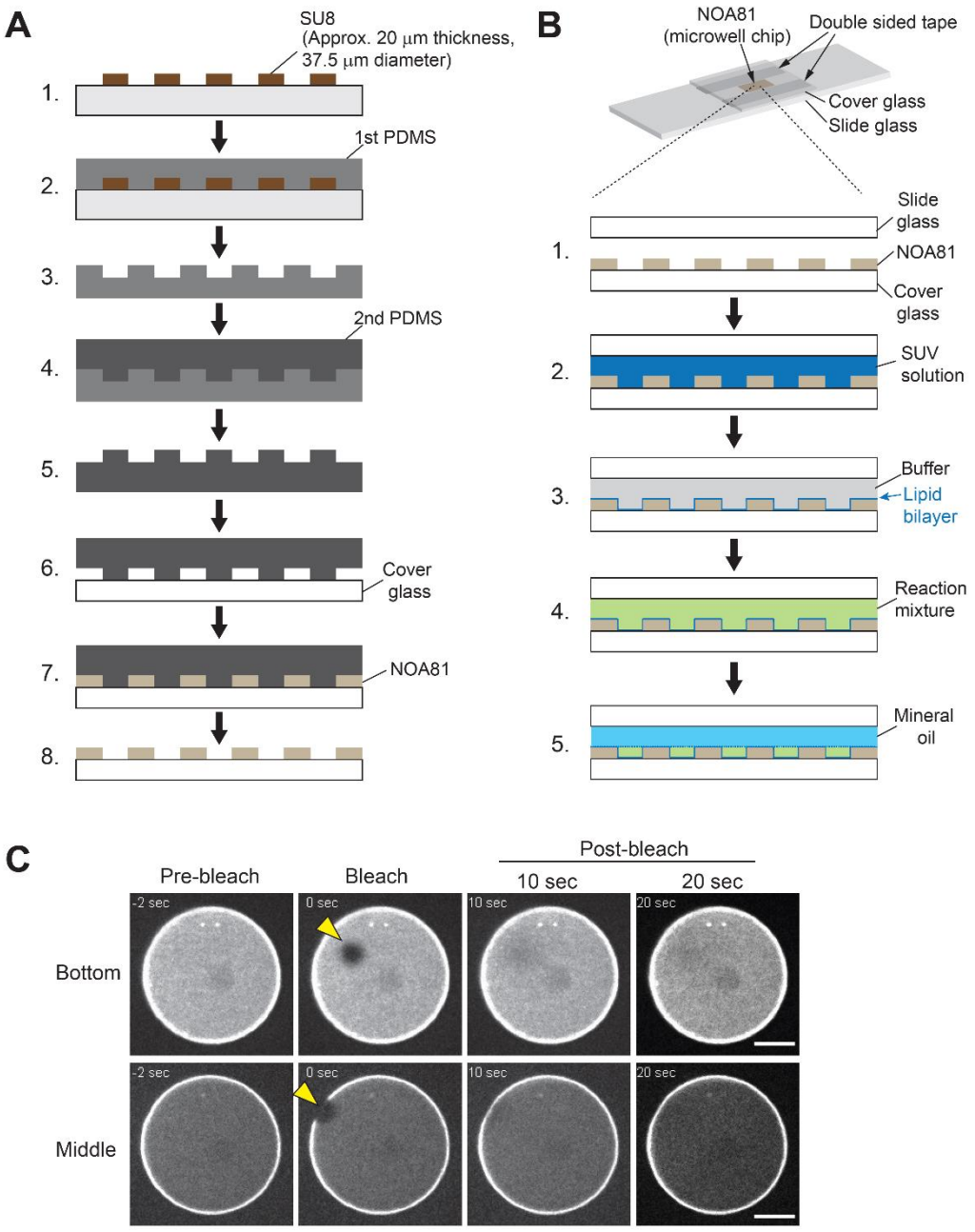

Appendix Fig. S1. Preparation of microwells and samples.

(A) Scheme of construction of NOA81-based microwells on a cover glass (See also Methods). SU8 mold was made on the wafer and silanized. The mold was used to make 1st PDMS mold. The 1st PDMS was silanized and then used to make 2nd PDMS. The 2nd PDMS was cut to small pieces and used as PDMS stamps. The PDMS stamp was placed on a cleaned cover glass. The space between pillars were filled with NOA81. By UV exposure, NOA81 was cured. The PDMS stamp and the excess NOA81 were removed. **(B)** Scheme of sample preparation (See also Methods). The NOA81-attached cover glass was exposed to plasma. After plasma treatment, the NOA81-attached cover glass was attached onto a

silane-PEG coated slide glass with double-sided tapes. Then, the SUV solution was loaded into the chamber and incubated to make a supported lipid bilayer on the surface of microwells. The excess SUVs were then removed from the chamber by perfusing with buffer solution. After washing, the chamber was filled with the reaction mixture containing tubulin and actin. Then, the microwells were immediately closed with mineral oil. **(C)** Photo-bleaching of lipids on microwell (Bottom or middle edge of the well). Fluorescently labelled lipids were photo-bleached (shown with yellow arrow head). Fluorescent recovery indicates diffusion of lipids. Scale bar 10 μm.

Appendix Fig. S2

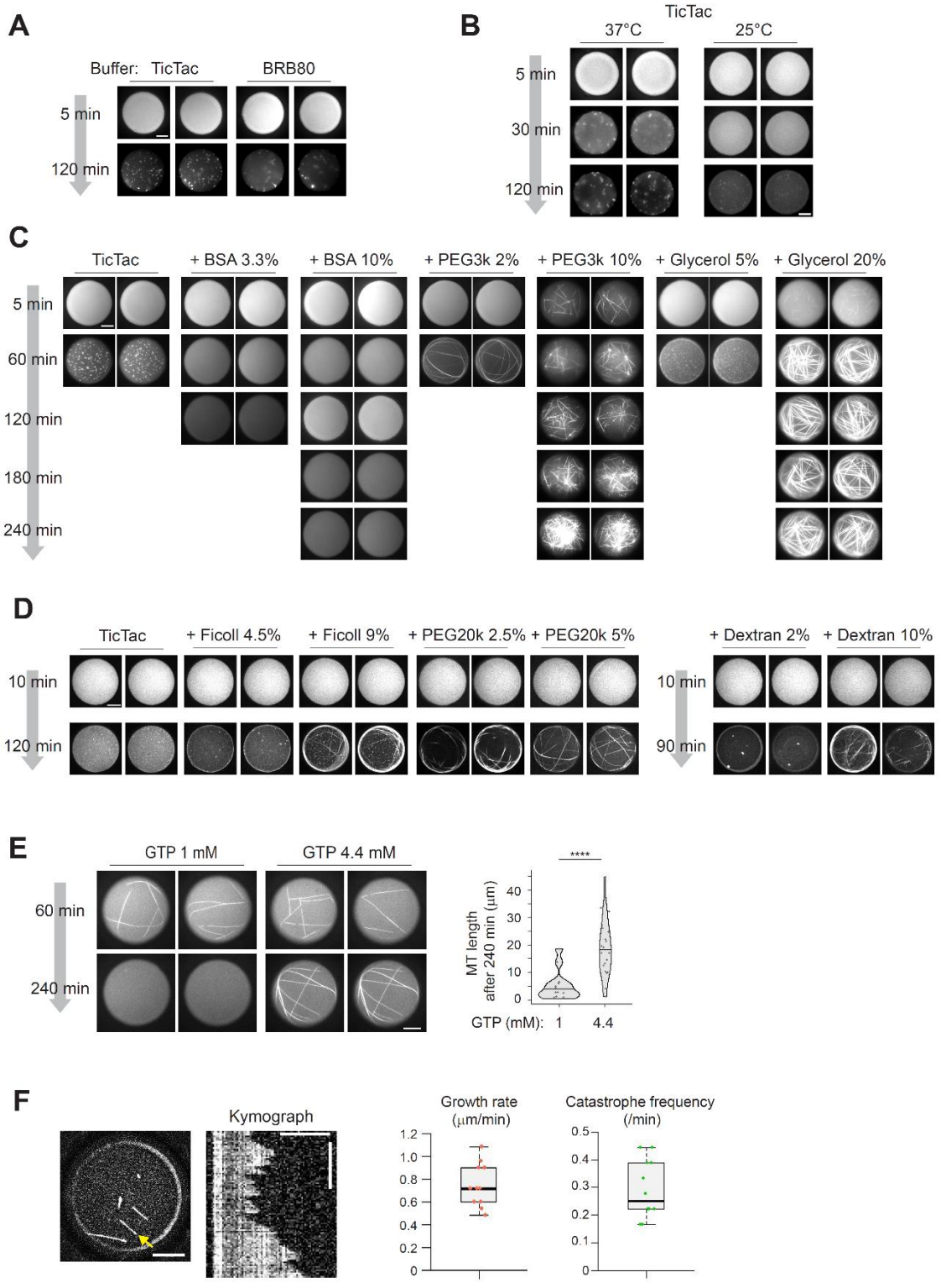

Appendix Fig. S2. Screening of biochemical conditions to slow down tubulin precipitation.

(A) Comparison of two different buffer solutions. Images show fluorescently labeled tubulin in microwells. Samples were incubated at 37°C after sample preparation. Tubulin 15 µM. Tubulin precipitation occurred both in the BRB80 and the TicTac buffer. **(B)** Comparison of two different

temperatures in the TicTac buffer. Images show fluorescently labeled tubulin in microwells. After sample preparation, samples were incubated at the indicated temperatures. Tubulin 20 μM. Incubation at lower temperature was better to slow down tubulin precipitation, although even at the lower temperature, tubulin precipitation occurred before 2 hours after sample preparation. **(C, D)** Test of various crowding reagents. Indicated reagents were added in the TicTac buffer. Images show fluorescently labeled tubulin in microwells. Samples were incubated at 25°C. Tubulin 12.5 μM. High concentration of BSA slowed down tubulin precipitation. Some of the crowding reagents (e.g. PEG) induced MT nucleation. The addition of PEG also induced tubulin aggregation, which resulted in the formation of aster-like structures. **(E)** Comparison of GTP concentrations. MT formation was induced by adding GMPCPP-stabilized MT seeds. Tubulin 8 μM. (GTP 1 mM n= 13, GTP 4.4 mM n = 20 MTs). Violin plots were shown with the median (horizontal line). ****p<0.0001 (Mann-Whitney U test). In this experiment, 15% BSA was added in the TicTac buffer. Addition of higher concentration of GTP maintained MTs for a long time. **(F)** MT dynamics in lipid coated microwells. Kymograph of the MT indicated by a yellow arrow was shown. GMPCPP-stabilized MT seeds were added to induce MT formation. Tubulin 16 μM. TicTac buffer supplemented with 5% BSA, 4.4 mM GTP, 2.7 mM ATP, 10 mM DTT, 20 μg/mL catalase, 3 mg/mL glucose, 100 μg/mL glucose oxidase. Samples were incubated at 22°C. Background subtraction was performed to increase signal-to-noise ratio. Scale bar 10 μm in larger image and 5 μm in kymograph, Time scale bar indicates 10 min in kymograph. n = 12 MTs; 2 independent experiments. Plots show box (25 to 75%) and whisker (10 to 90%). Lines in the box indicate medians. Data information: **(A)-(E)** Images of wells were randomly taken at each time point, indicating that the represented wells were not identical through time points. In these experiments, microwells were coated with Silane-PEG30k. As a basic buffer solution (control), BRB80 or TicTac buffer supplemented with 0.1% BSA, 1 mM GTP, 2.7 mM ATP, 20 mM DTT, 20 μg/mL catalase, 3 mg/mL glucose, 100 μg/mL glucose oxidase was used. Scale bar 10 μm.

Appendix Fig. S3

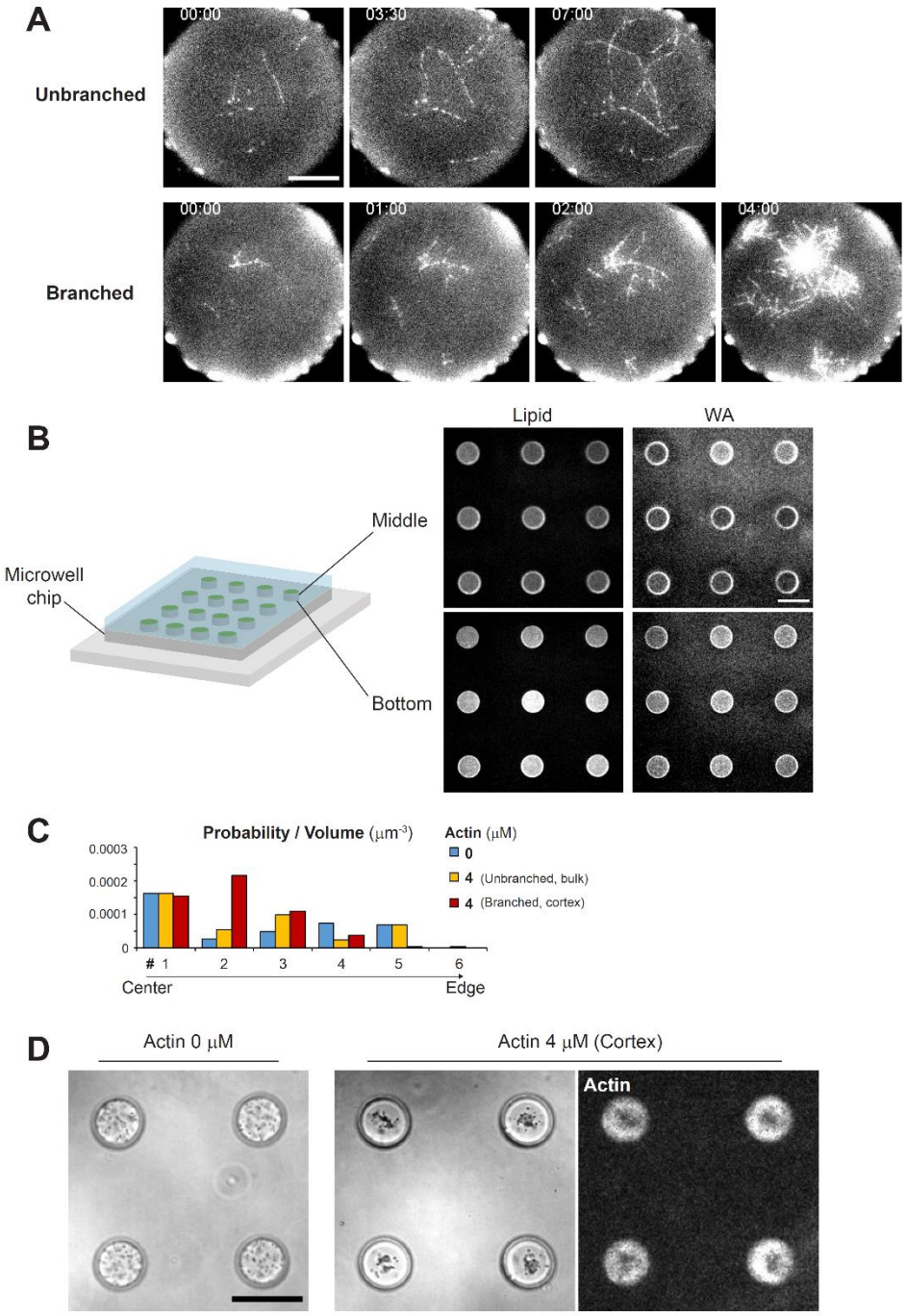

Appendix Fig. S3. Characterization of actin assembly in microwells.

(A) Time-lapse imaging of actin assembly on lipid coated microwells by TIRF microscope. Top images show unbranched actin (Actin 1.25 μM). Bottom images show branched actin (Actin 1.25 μM, Arp2/3 complex 80 nM, GST-WA 100 nM). In these experiments, 0.25% of methyl cellulose (Sigma, 1500 cP) was added to visualize actin filaments within the TIRF field. Time indicates (min:sec). Scale bar 10 μm. **(B)** Lipid and NPF (WA) coated microwells. Fluorescence labelled lipid and snap-streptavidin-WA were used. Scale bar 50 μm. **(C)** Distribution of the aMTOC in the absence of free tubulin in

microwells. Probability per volume was calculated as shown in Figure EV2A. Data shown in Figure 2E were used. **(D)** Distribution of smaller beads (1 μm in diameter, PolySciences, #08226) in the absence or presence of cortical actin (Actin 4 μM, Arp2/3 80 nM and NPF coating) in microwells. In bright field images, black dots in microwells indicate the beads. The presence of cortical actin clustered the beads to the well center. Scale bar, 50 μm.

Appendix Table S1

Cytosim parameters

		Value	Note
Global	Time step	0.01 s	Computational parameter
	Viscosity	0.3 pN s/μm^2	(Ref S1)
	Steric force constant (Repulsion)	1.5 pN/μm	Adapted from the range in previous studies (Ref S2, S3)
Cell	Radius	10 μm	Radius for the basic circular geometry (Ref S4)
	Confinement stiffness	500 pN/μm	Confinement strength of microtubules and actin filaments inside the cell (Ref S4)
Microtubule	Rigidity	25 pN μm^2	Persistence length Lp = 5200 μm (Red S4, S5)
	Segmentation	0.2 μm	Computational parameter
	Steric radius	50 nm	(Ref S2, S3)
	Growing speed	Varied	(Ref S4, S6)
	Stall force	1.67 pN	Growing sensitivity to force (Ref S7, S8)
	Shrinking speed	0.27 μm/s	(Ref S4, S6)
	Catastrophe rate	0.01, 0.04 s^{-1}	Unloaded and stalled catastrophe rate (Ref S4, S9)
	Rescue rate	0.064 s^{-1}	(Ref S4, S6)
	Initial length	1 μm	Length of microtubules at t=0 sec
MTOC	Radius	0.5 μm	Radius of MTOC (Ref S4)
	First anchoring stiffness	500 pN/μm	Stiffness of the link anchoring microtubules to the center of MTOC (Ref S4)
	Second anchoring stiffness	500 pN/μm	Stiffness of the link anchoring microtubules to a point on the MTOC periphery (Ref S4)
Actin	Rigidity	0.06 pN μm^2	Persistence length Lp = 15 μm was chosen. (Ref S2, S10)
	Segmentation	0.2 μm	Computational parameter
	Steric radius	50 nm	(Ref S2, S3)
Bulk actin network			

Actin	Number	Varied	Number of actin filaments
	Length	5 μm	Length of actin filaments

Actin near cell periphery

Actin nucleation factor	Nucleation rate	100 s^{-1}	Rate of nucleation, High enough for quick actin assembly
	Length of actin filaments	2 μm	
	Unbinding rate	0 s^{-1}	No detachment
	Stiffness	100 pN/μm	Stiffness of the link between the nucleator and its fixed anchoring position
	Number	Varied	Number of actin nucleation factor
Actin branching factor	Nucleation rate	100 s^{-1}	Nucleation rate when bound to an existing filament, for quick actin assembly
	Length of actin filaments	1 μm	
	Binding rate	1 s^{-1}	Binding rate for quick actin assembly
	Binding range	0.01 μm	Bind to a close filament
	Unbinding rate	0 s^{-1}	No detachment
	Equilibrium angle	1.22 rad	Angle between the two branches, 70° (Ref S11)
	Angular stiffness	0.13 pN.μm/rad	Stiffness of the torque connecting the two branches (Ref S2, S11)
	Diffusion	0 $\mu m^2/s$	No diffusion, in order to limit the region of actin assembly
	Number	Varied	Number of actin branching factor

Varying parameters

		Value	Figures	Note
Microtubule	Number of microtubules	90	Except for Fig.EV3F, EV4G and EV5I	Number of microtubules at t=0 sec
		30	Fig.EV3F, EV4G and EV5I	

	Growing speed	0.07 μm/s	Fig.3E-G Fig.EV3D-F	Aster with shorter MTs
		0.13 μm/s	Fig.4K-M, 5K-M Fig.EV4F, G, J and EV5H, I	(Ref S4, S6)
Actin (Bulk actin)	Number	800	Fig.3E-G, Fig.EV3D, F	Dense actin filaments (Bulk)
		80	Fig.EV3E	Loose actin filaments (Buk)
Actin nucleation factor	Number	1400	Fig.4K-M Fig.EV4F, G	Symmetric actin network (periphery)
		905	Fig.5K-M, Fig.EV5H, I	Asymmetric actin network (periphery)
		100	Fig.EV4J	Loose actin network (Periphery)
Actin branching factor	Number	2100	Fig.4K-M Fig.EV4F, G	Symmetric actin network (periphery)
		365	Fig.5K-M, Fig.EV5H, I	Asymmetric actin network (periphery)
		100	Fig.EV4J	Loose actin network (Periphery)

References in Appendix Table S1

S1. Polyakov, O. Y. (2013). Mechanical Aspects of Drosophila Gastrulation. Princeton University

S2. Letort, G., Politi, A. Z., Ennomani, H., Théry, M., Nedelec, F., & Blanchoin, L. (2015). Geometrical and Mechanical Properties Control Actin Filament Organization. *PLOS Computational Biology*, *11*(5), e1004245. https://doi.org/10.1371/JOURNAL.PCBI.1004245

S3. Rickman, J., Nédélec, F., & Surrey, T. (2019). Effects of spatial dimensionality and steric interactions on microtubule-motor self-organization. *Physical Biology*, *16*(4), 046004. https://doi.org/10.1088/1478-3975/ab0fb1

S4. Letort, G., Nedelec, F., Blanchoin, L., & Théry, M. (2016). Centrosome centering and decentering by microtubule network rearrangement. *Molecular Biology of the Cell*, *27*(18), 2833–2843. https://doi.org/10.1091/mbc.E16-06-0395

S5. Gittes, F., Mickey, B., Nettleton, J., & Howard, J. (1993). Flexural rigidity of microtubules and actin filaments measured from thermal fluctuations in shape. *Journal of Cell Biology*, *120*(4), 923–934. https://doi.org/10.1083/jcb.120.4.923

S6. Burakov, A., Nadezhdina, E., Slepchenko, B., & Rodionov, V. (2003). Centrosome positioning in interphase cells. *Journal of Cell Biology*, *162*(6), 963–969. https://doi.org/10.1083/jcb.200305082

S7. Dogterom, M., & Yurke, B. (1997). Measurement of the force-velocity relation for growing microtubules. *Science*, *278*(5339), 856–860. https://doi.org/10.1126/SCIENCE.278.5339.856

S8. Kozlowski, C., Srayko, M., & Nedelec, F. (2007). Cortical Microtubule Contacts Position the Spindle in C. elegans Embryos. *Cell*, *129*(3), 499–510. https://doi.org/10.1016/j.cell.2007.03.027

S9. Janson, M. E., De Dood, M. E., & Dogterom, M. (2003). Dynamic instability of microtubules is regulated by force. *Journal of Cell Biology*, *161*(6), 1029–1034. https://doi.org/10.1083/jcb.200301147

S10. Isambert, H., Venier, P., Maggs, A. C., Fattoum, A., Kassab, R., Pantaloni, D., & Carlier, M. F. (1995). Flexibility of Actin Filaments Derived from Thermal Fluctuations. Effect of bound nucleotide, phalloidin, and muscle regulatory proteins. *Journal of Biological Chemistry*, *270*(19), 11437–11444. https://doi.org/10.1074/JBC.270.19.11437

S11. Blancholn, L., Amann, K. J., Higgs, H. N., Marchand, J. B., Kaiser, D. A., & Pollard, T. D. (2000). Direct observation of dendritic actin filament networks nucleated by Arp2/3 complex and WASP/Scar proteins. *Nature*, *404*(6781), 1007–1011. https://doi.org/10.1038/35010008